Communication

Ion Motion in Conjugated Polyelectrolyte Electron Transporting Layers

Corey Hoven, Renqiang Yang, Andres Garcia, Alan J. Heeger, Thuc-Quyen Nguyen, and Guillermo C. Bazan

J. Am. Chem. Soc., **2007**, 129 (36), 10976-10977• DOI: 10.1021/ja072612q • Publication Date (Web): 17 August 2007

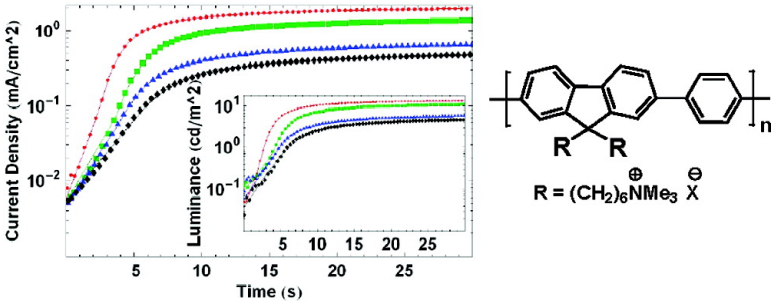

More About This Article

Additional resources and features associated with this article are available within the HTML version:

- Supporting Information
- Links to the 12 articles that cite this article, as of the time of this article download
- Access to high resolution figures
- Links to articles and content related to this article
- Copyright permission to reproduce figures and/or text from this article

View the Full Text HTML

J|A|C|S
COMMUNICATIONS

Published on Web 08/17/2007

Ion Motion in Conjugated Polyelectrolyte Electron Transporting Layers

Corey Hoven, Renqiang Yang, Andres Garcia, Alan J. Heeger, Thuc-Quyen Nguyen,* and Guillermo C. Bazan*

Department of Chemistry & Biochemistry, Department of Materials, Institute for Polymers and Organic Solids, University of California, Santa Barbara, California 93106

Received April 14, 2007; E-mail: quyen@chem.ucsb.edu; bazan@chem.ucsb.edu

In organic light-emitting diodes (OLEDs), electrons are injected from the cathode into the π^*-band (lowest unoccupied molecular orbital) of an organic semiconductor and holes are injected from the anode into the π-band (highest occupied molecular orbital). If the work function of the cathode is greater than the π^*-band or the work function of the anode is less than the π-band, these differences lead to charge injection barriers. Because of these barriers the current is limited to a first approximation by a combination of Fowler−Nordheim tunneling and thermionic emission mechanisms.[1] These barriers reduce device power efficiencies by increasing the turn on voltage and creating unbalanced charge injection. This problem provides a substantial obstacle to using OLEDs in solid-state lighting applications.

A challenge thus lies in reducing the electron injection barrier. Using low work function metals, such as Ca or Ba, can effectively reduce the barrier, but these metals tend to be environmentally unstable, which lowers device lifetime, and require strict encapsulation processes. OLEDs with multiple layer architectures can display improved efficiencies.[2] Electron transport/injection layers (ETLs) reduce the electron injection barrier by a variety of mechanisms, including placing a dipole adjacent to the cathode,[3] band bending using doped ETLs to create ohmic contacts,[4] or through a series of energetically cascading layers.[5] ETLs with high electron mobilities can move the charge recombination region away from the cathode, where excitons can be quenched.[6] ETLs can also be used as blocking layers that prevent holes from migrating across the device without recombining, forces the recombination profile away from the cathode, and alters the internal field distribution.[7]

Polymer LEDs (PLEDs) offer the opportunity of device fabrication using solution methods. However, multilayer fabrication is challenging if all the components display similar solubility characteristics. Depositing a new polymer layer can lead to removal of the underlying layer and/or mixing of the components.[8] Conjugated polyelectrolytes are helpful in this context since their charged groups increase their solubility in polar solvents, such as water or methanol. The differences in solubility, compared to neutral conjugated polymers, are advantageous for fabricating the desired multilayer architectures. Additionally, by using conjugated polyelectrolytes as the ETL one can circumvent the restrictions of having to match cathode work function to the semiconductor energy level.[9,10]

Despite the successful application of conjugated polyelectrolytes as ETLs, the exact mechanism by which electron injection barriers are reduced remains poorly understood. It has been proposed that a permanent dipole between the cathode and the polymer lowers the injection barrier,[11] possibly due to self-assembly and alignment of the polymer at the interface.[12] However, it has also been shown that the nature of the charge compensating ion also influences the turn-on voltage of the device and the maximum efficiency.[13,14] In this contribution we reveal that the reduction in the injection barrier involves a rearrangement of the counterions within the ETL under the applied bias.

Scheme 1. Device Structure and Molecular Structure of PFN-BIm_4

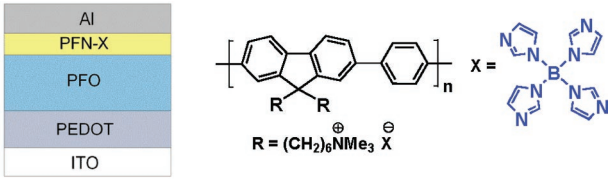

The device test structures used for our measurements (Scheme 1) were fabricated by spin casting a chlorobenzene solution of poly(9,9-dioctylfluorenyl-2,7-diyl) (PFO) on top of an ITO electrode that was cleaned, UV/ozone treated, and then passivated with 80 nm of poly(3,4-ethylenedioxythiophene)-poly(styrenesulfonate) (PEDOT). The resulting PFO thickness was approximately 100 nm, as determined by atomic force microscopy (AFM) measurements. After the structure was annealed at 120 °C for 30 min, a layer of poly[9,9′-bis[6″-(*N*,*N*,*N*-trimethylammonium)hexyl] fluorene-*alt*-*co*-phenylene] (PFN, see Scheme 1 for molecular structure) with tetrakis(imidazolyl)borate (BIm_4) counterions was deposited from methanol to serve as the ETL. This counterion was previously shown to give excellent performance in related PLEDs.[14] The PFN-BIm_4 thickness was controlled by varying the spin rate and was measured using profilometry by comparison with a control PEDOT/PFO layer. Before applying the Al cathode by evaporation at 10^{-6} Torr, the devices were kept under vacuum at 10^{-4} Torr for 12 h to remove solvents. Fabrication and testing were carried out inside a N_2 atmosphere drybox.

Figure 1a shows how the current density (J) develops over time at different applied voltages for a device containing a 10 nm thick PFN-BIm_4 layer. A low current is initially observed, which increases up to a limiting value. Faster response times and higher steady state J values are attained when the applied voltage is increased. Defining the response time as the time when J is 50% of its maximum value, the transients in Figure 1a have response times of 0.5 s for 6 V, 2.5 s for 5 V, 6.1 s for 4.5 V, and 20 s for 4 V. The luminance (L) characteristics for these devices are shown in Figure 1b. Similar behavior to the J vs time response is observed: higher brightness and lower response times occur as one increases the applied bias. Lowering electron injection barriers leads to higher current densities and more excitons via charge recombination events.

Also shown in Figure 1 are the characteristics of a device without PFN-BIm_4 at an applied bias of 5 V, that is, the Al cathode was deposited on the PFO layer. Under these conditions one observes no significant emission and a current density that is over 2 orders of magnitude smaller than that obtained with the ETL layer and invariant after the first measurement is taken (approximately 80 ms). The primary action of PFN-BIm_4 is thus to improve electron injection.

10.1021/ja072612q CCC: $37.00

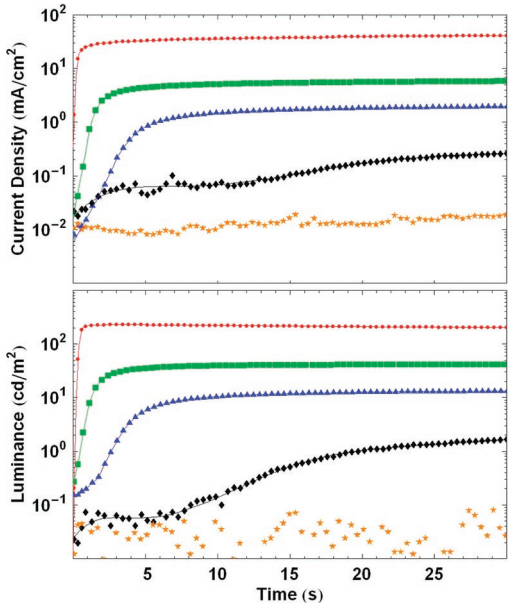

Figure 1. Time response of J and L for a ITO/PEDOT/PFO/PFN-BIm$_4$/Al LED with constant applied bias: 6 V (red circles), 5 V (green squares), 4.5 V (blue triangles), 4 V (black diamonds). Shown in orange stars are the data from a device without the PFN-BIm$_4$ layer at 5 V.

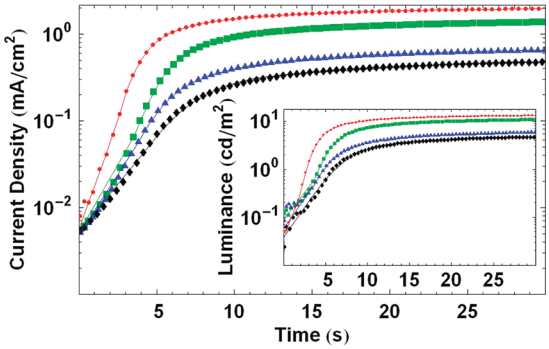

Figure 2. Time response of J and L (inset) for a ITO/PEDOT/PFO/PFN-BIm$_4$/Al LED with 4.5 V applied with different PFN-BIm$_4$ thicknesses: 10 nm (red circles), 15 nm (green squares), 25 nm (blue triangles), 30 nm (black diamonds).

Figure 2 shows the J vs time and L vs time (inset) responses at an applied bias of 4.5 V for devices with different PFN-BIm$_4$ layer thicknesses. A current of about 0.005 mA/cm^2 is observed after 80 ms, which increases up to saturation values of 2.4 , 1.75, 0.93, and 0.67 mA/cm^2 when the PFN-BIm$_4$ layer thicknesses are 10, 15, 25, and 30 nm, respectively. The response times increase with layer thickness: 6.1 s for 10 nm, 8.2 s for 15 nm, 9.2 s for 25 nm, and 10.4 s for 30 nm. The total electric fields across the different devices do not change considerably. For the thinnest device (10 nm ETL) the field is 4.1×10^5 V/cm, while for the thickest device (30 nm ETL) the corresponding field is 3.5×10^5 V/cm. After a relaxation time of 60 min or greater, one observes similar time responses. Altogether, the data show that the thicker the ETL is, the longer is the response time and the lower is the steady state J and L and that the changes are reversible.

The observation of a time response for J in the regime of seconds, together with the similar time response for L, upon introduction of the PFN-BIm$_4$ layer are consistent with ion motion mediating the device performance and, in particular, the electron injection barrier. Such dependence is difficult to accommodate within a model where the effective workfunction of the cathode is modified by the presence of a permanent dipole at the conjugated polyelectrolyte interface. In conventional PLEDs the electroluminescent response is on the nanosecond or microsecond time scales.[15,16] For example, PFO LEDs with Ca cathodes have voltage dependent response times on the order of microseconds.[17]

It is useful to note here that conjugated polyelectrolytes have also been used successfully as the active layer in single component light-emitting electrochemical cells (LECs).[18] In LECs, the ion motion redistributes the field within the device[19] and compensates the injected charges.[20] There is field-driven displacement of anions away from the cathode. The response time in LECs is affected by the mobility of the ions, the distance the ions must traverse, and the magnitude of the electric field,[21] very much like the dependence shown in Figures 1 and 2. The action of the polyelectrolyte ETL thus leads to a hybrid device that combines features of PLEDs and LECs and involves mixed ionic and electronic conduction. The time response due to ion motion may provide challenges in nonstatic displays but should not be a significant concern when considering white emitting PLEDs for solid-state lighting applications.

Acknowledgment. We are grateful to NSF (Grant DMR 0606414 and DMR 0547639) and the Materials Research Laboratory for financial support.

References

(1) Parker, I. D. *J. Appl. Phys.* **1994**, *75*, 1665.
(2) Tang, C. W.; Vanslyke, S. A. *Appl. Phys. Lett.* **1987**, *51*, 913.
(3) Ishii, H.; Sugiyama, K.; Ito, E.; Seki, K. *Adv. Mater.* **1999**, *11*, 605.
(4) Shen, Y. L.; Hosseini, A. R.; Wong, M. H.; Malliaras, G. G. *Chem. Phys. Chem.* **2004**, *5*, 16.
(5) Nuyken, O.; Jungermann, S.; Wiederhirn, V.; Bacher, E.; Meerholz, K. *Monatsh. Chem.* **2006**, *137*, 811.
(6) Malliaras, G. G.; Scott, J. C. *J. Appl. Phys.* **1998**, *83*, 5399.
(7) Campbell, I. H.; Joswick, M. D.; Parker, I. D. *Appl. Phys. Lett.* **1995**, *67*, 3171.
(8) Steuerman, D. W.; Garcia, A.; Yang, R.; Nguyen, T.-Q. *Adv. Mater.*, in press.
(9) Gong, X.; Wang, S.; Moses, D.; Bazan, G. C.; Heeger, A. J. *Adv. Mater.* **2005**, *17*, 2053.
(10) Ma, W. L.; Iyer, P. K.; Gong, X.; Liu, B.; Moses, D.; Bazan, G. C.; Heeger, A. J. *Adv. Mater.* **2005**, *17*, 274.
(11) Shen, H. L.; Huang, F.; Hou, L. T.; Wu, H. B.; Cao, W.; Yang, W.; Cao, Y. *Synth. Met.* **2005**, *152*, 257.
(12) Wu, H. B.; Huang, F.; Peng, J. B.; Cao, Y. *Org. Electron.* **2005**, *6*, 118.
(13) Yang, R. Q.; Garcia, A.; Korystov, D.; Mikhailovsky, A.; Bazan, G. C.; Nguyen, T. Q. *J. Am. Chem. Soc.* **2006**, *128*, 16532.
(14) Yang, R. Q.; Wu, H. B.; Cao, Y.; Bazan, G. C. *J. Am. Chem. Soc.* **2006**, *128*, 14422.
(15) Book, K.; Nikitenko, V. R.; Bassler, H.; Elschner, A. *Synth. Met.* **2001**, *122*, 135.
(16) Wang, J.; Sun, R. G.; Yu, G.; Heeger, A. J. *Synth. Met.* **2003**, *137*, 1009.
(17) Pinner, D. J.; Friend, R. H.; Tessler, N. *J. Appl. Phys.* **1999**, *86*, 5116.
(18) (a) Cheng, C. H. W.; Lin, F. D.; Lonergan, M. C. *J. Phys. Chem. B* **2005**, *109*, 10168. (b) Cimrova, V.; Schmidt, W.; Rulkens, R.; Schulze, M.; Meyer, W.; Neher, D. *Adv. Mater.* **1996**, *8*, 585. (c) Edman, L.; Liu, B.; Vehse, M.; Swensen, J.; Bazan, G. C.; Heeger, A. J. *J. App. Phys.* **2005**, *98*, 44502. (d) Gu, Z.; Shen, Q. D.; Zhang, J.; Yang, C. Z.; Bao, Y. J. *J. Appl. Polym. Sci.* **2006**, *100*, 2930. (e) Neher, D.; Gruner, J.; Cimrova, V.; Schmidt, W.; Rulkens, R.; Lauter, U. *Polym. Adv. Technol.* **1998**, *9*, 461.
(19) deMello, J. C.; Tessler, N.; Graham, S. C.; Friend, R. H. *Phys. Rev. B* **1998**, *57*, 12951.
(20) (a) Pei, Q. B.; Yu, G.; Zhang, C.; Yang, Y.; Heeger, A. J. *Science* **1995**, *269*, 1086. (b) Smith, D. L. *J. Appl. Phys.* **1997**, *81*, 2869.
(21) (a) Pei, Q. B.; Yang, Y.; Yu, G.; Zhang, C.; Heeger, A. J. *J. Am. Chem. Soc.* **1996**, *118*, 3922. (b) Zhang, Q. S.; Zhou, Q. G.; Cheng, Y. X.; Wang, L. X.; Ma, D. G.; Jing, X. B.; Wang, F. S. *Adv. Funct. Mater.* **2006**, *16*, 1203.

JA072612Q